

## Para-ortho transition of artificial H<sub>2</sub> molecule in lateral quantum dots doped with magnetic impurities

Ramin M. Abolfath

Department of Radiation Oncology, University of Texas Southwestern Medical Center, Dallas, Texas 75390, USA  
(Received 25 September 2009; published 27 October 2009)

We present the magnetic phase diagram of artificial H<sub>2</sub> molecule in lateral quantum dots doped with magnetic impurities as a function of external magnetic field and plunger gate voltage. The onset of Mn-Mn antiferromagnetic-ferromagnetic transition follows the electron spin singlet-triplet transition. We deploy a configuration-interaction method to exactly diagonalize the electron-Mn Hamiltonian and map it to an effective Mn-Mn Heisenberg Hamiltonian. We find that Mn-Mn exchange coupling can be described by RKKY-interaction/magnetic-polaron in weak/strong electron-Mn coupling at low/high magnetic fields.

DOI: [10.1103/PhysRevB.80.165332](https://doi.org/10.1103/PhysRevB.80.165332)

PACS number(s): 73.43.Lp, 73.63.Kv, 75.50.Gg

### I. INTRODUCTION

There is currently significant experimental<sup>1-7</sup> and theoretical<sup>8-14</sup> interest in semiconductor quantum dots (QDs) doped with magnetic impurities. Fabrication of hybrid systems consisting magnetic ions in a controlled electronic environment provides an interesting interplay between interaction effects and magnetism. In particular, the application of spin of electrons in quantum dot molecules for generation of electron entanglement and quantum information processing in solid state devices is of current interest.<sup>15,16</sup> One of the challenges in use of spin of electrons in scalable quantum computer devices is the spin dephasing due to interference by spin-orbit coupling and nuclear hyperfine interaction.<sup>17</sup> The broadening of the electron envelope wave function in a QD is determined by the length scale of the confining potential that is comparable with the size of QD (typically  $\approx 1-1000$  nm). In materials with high abundance of spin-carrying nuclear isotopes, the electron interacts with large number of nuclei in host semiconductor. Although the strength of nuclear hyperfine coupling is small (typically  $\approx 1 \mu\text{eV}$ ) compared to other relevant energy scales, but because of the broadening of the confined electron in nanometer length scale, it interacts with a large number of nuclei that contribute to the electron spin dephasing. The use of magnetic moment of nuclear impurities in host semiconductors for the quantum information processing have appeared to overcome this limitation.<sup>18,19</sup> To avoid such problem, it has been suggested that the magnetic moment of nucleus of host semiconductor constituents (atoms and impurities) to be used extensively for the quantum information processing.<sup>18,19</sup> Recently the system of <sup>13</sup>C atoms in two-electron nanotube quantum dot molecule has been studied.<sup>20</sup> The advantage of using singlet eigenstates of coupled magnetic moments of nucleus of <sup>13</sup>C in organic molecules and their effects in dramatic enhancement of the spin lifetimes needed for imaging the metabolic pathways in living systems by hyperpolarization methods has been investigated.<sup>21</sup> Moreover, molecules doped with <sup>13</sup>C has been used in demonstration of quantum teleportation using nuclear magnetic resonance techniques.<sup>18</sup> Similarly the magnetic dipole moment of nucleus of <sup>31</sup>P impurities in Si-based quantum computer model proposed by Kane<sup>19</sup> appears to be promising in making quantum com-

puter solid state devices. Similar to magnetic dipole moment of nucleus of <sup>13</sup>C and/or <sup>31</sup>P, the magnetic moment of electrons in *d* shell of magnetic impurities (such as Mn, Fe, and Co) in lateral quantum dot molecules can be used for quantum information processing as they have been used for fabrication of molecular magnets.<sup>22</sup>

In this work, we focus on theoretical study of the phase diagram and spin transitions of coupled magnetic impurities (e.g., Mn) doped in two electron quantum dot molecule, an artificial H<sub>2</sub> molecule. Here, we calculate the Mn-Mn effective Hamiltonian mediated by electrons and show that the onset of spin-polarized state with finite Mn magnetization, corresponds to spin singlet-triplet transition of two electrons in QD molecule. This transition is analogous to para-ortho transition of nucleus of solid H<sub>2</sub> where the electron-nuclei hyperfine interaction opens the energy gap between para and ortho states of H<sub>2</sub> molecule.<sup>24,25</sup> In the small (large) magnetic fields the spin-singlet (triplet) state is the ground state of electrons<sup>16</sup> and thus the ground state of the coupled Mn is described by hydrogen molecule para (ortho) state. In the small magnetic fields, the Mn-Mn interaction induced by electrons is calculated perturbatively in the electron-Mn weak interacting limit. It can be described effectively by RKKY-coupling.<sup>23</sup> In large magnetic field, the ground state of electrons is spin-triplet. The electron-Mn interaction is strong and magnetic-polaron state form. In this limit the ortho-state of artificial H<sub>2</sub> molecule is stable. We show the Mn-Mn exchange coupling can be controlled by inter- and intradot correlations, external magnetic field, and gate voltage.

The dependence of Mn-Mn interaction to the spin singlet-triplet transition among electrons in QDs opens up the possibility in using Mn-magnetic moment as qubit in quantum computation purposes. In contrast to electrons confined in QD's, because of highly localized *d* electrons, Mn's interact directly with significantly smaller number of nuclei of host semiconductor. The Mn *d* electrons also do not interact directly with the host semiconductor Rashba and Dresselhaus spin-orbit coupling,<sup>28</sup> and thus their spin coherence life-time is expected to be longer than the QD electrons. However, Mn-Mn interaction mediated by electrons in QDs is still vulnerable to the electron spin dephasing mediated by QD electrons due to their hyperfine and spin-orbit couplings. In

analogous to the  $^{31}\text{P}$  in Si system,<sup>19</sup> the spin coherence time in the Mn system is expected to be longer than the QD electron system. Further investigation is required to make a quantitative dependence of spin decoherence time of Mn on the electron-nuclear hyperfine interaction and their spin-orbit coupling.

## II. HAMILTONIAN

We represent magnetic QD molecule by the Hamiltonian  $H=H_e+H_{em}+H_m$ , describing contributions of interacting electrons, electron-Mn ( $e$ -Mn) exchange, and direct Mn-Mn antiferromagnetic (AFM) coupling, respectively. Electrons confined in quasi-two-dimensional quantum dots in a uniform perpendicular magnetic field can be described by the effective mass Hamiltonian

$$H_e = \sum_{i=1}^N (T_i + E_{iz}) + \frac{e^2}{2\epsilon} \sum_{i \neq j} \frac{1}{|\vec{r}_i - \vec{r}_j|}, \quad (1)$$

where

$$T = \frac{1}{2m^*} \left( \frac{\hbar}{i} \vec{\nabla} + \frac{e}{c} A(\vec{r}) \right)^2 + V(x, y) \quad (2)$$

is the single electron Hamiltonian in magnetic field. Here,  $(\vec{r})=(x, y)$  describes electron position,  $V(\vec{r})$  is the quantum dots confining potential,  $A(\vec{r})=\frac{1}{2}\vec{B} \times \vec{r}$  is the vector potential, and  $B$  is the external magnetic field perpendicular to the plane of confining potential.  $m^*$  is the conduction-electron effective mass,  $-e$  is the electron charge, and  $\epsilon$  is the host semiconductor dielectric constant.  $E_{iz}=\frac{1}{2}g_e\mu_B\sigma_{iz}B$  is the Zeeman spin splitting,  $g_e$  is the electron  $g$  factor in host semiconductor,  $\mu_B$  is the Bohr magneton, and  $\sigma$  is the Pauli matrix. The single-particle eigenvalues ( $\epsilon_{\alpha\sigma}$ ) and eigenvectors ( $\varphi_{\alpha\sigma}$ ) are calculated by discretizing  $T$  in real space, and diagonalizing the resulting matrix using conjugated gradient algorithm.<sup>16,26</sup> The single-particle (SP) states can be used as a basis in configuration-interaction (CI) calculation that allows to diagonalize Hamiltonian  $H$ . The details of CI method can be found in Ref. 26. Denoting the creation (annihilation) operators for electron in noninteracting SP state  $|\alpha\sigma\rangle$  by  $c_{\alpha\sigma}^\dagger$  ( $c_{\alpha\sigma}$ ), the Hamiltonian of an interacting system in second quantization can be written as

$$H_e = \sum_{\alpha} \sum_{\sigma} \epsilon_{\alpha\sigma} c_{\alpha\sigma}^\dagger c_{\alpha\sigma} + \frac{1}{2} \sum_{\alpha\beta\gamma\mu} \sum_{\sigma\sigma'} V_{\alpha\sigma, \beta\sigma', \gamma\sigma', \mu\sigma} c_{\alpha\sigma}^\dagger c_{\beta\sigma'}^\dagger c_{\gamma\sigma'} c_{\mu\sigma}, \quad (3)$$

where the first term represents the single-particle Hamiltonian Eq. (2), and  $V_{\alpha\sigma, \beta\sigma', \gamma\sigma', \mu\sigma} = \int d\vec{r} \int d\vec{r}' \varphi_{\alpha\sigma}^*(\vec{r}) \varphi_{\beta\sigma'}^*(\vec{r}') \frac{e^2}{|\vec{r}-\vec{r}'|} \varphi_{\mu\sigma'}(\vec{r}') \varphi_{\nu\sigma}(\vec{r})$ , is the two-body Coulomb matrix element. We describe  $e$ -Mn exchange interaction by  $H_{em}=-J_{sd}\sum_i \vec{s}_i \cdot \vec{M}_I \delta(\mathbf{r}_i - \mathbf{R}_I)$ , where  $J_{sd}$  is the exchange coupling between electron spin  $\vec{s}_i$  at  $\mathbf{r}_i$  and impurity spin  $\vec{M}_I$  at  $\mathbf{R}_I$ .<sup>10,11</sup> Note that  $H_{em}$  is analogous of the isotropic (contact) part of electron-nucleus hyperfine

interaction,<sup>27</sup> responsible for para-ortho energy gap of solid  $H_2$  (for comparison see, for example, Eq. 121.9, page 498 of Ref. 24). In second quantization it can be written as

$$H_{em} = - \sum_{\alpha\beta} \sum_I \frac{J_{\alpha\beta}(\mathbf{R}_I)}{2} [M_{zI} (c_{\alpha\uparrow}^\dagger c_{\beta\uparrow} - c_{\alpha\downarrow}^\dagger c_{\beta\downarrow}) + M_I^+ c_{\alpha\downarrow}^\dagger c_{\beta\uparrow} + M_I^- c_{\alpha\uparrow}^\dagger c_{\beta\downarrow}], \quad (4)$$

where  $J_{\alpha\beta}(\mathbf{R}_I)=J_{sd}\varphi_{\alpha}^*(\mathbf{R}_I)\varphi_{\beta}(\mathbf{R}_I)$ . Finally we describe Mn-Mn direct exchange interaction and Mn-Zeeman coupling by  $H_m=\sum_{I,I'} J_{I,I'}^{AF} \vec{M}_I \cdot \vec{M}_{I'} + \sum_I g_m \mu_B M_{zI} B$ , where  $J_{I,I'}^{AF}$  is the direct Mn-Mn AFM coupling,<sup>10</sup> resembling the direct dipole-dipole interaction, and  $g_m$  is the Mn  $g$  factor.

## Confining potential

For numerical calculation, we model quantum dots molecules by the following confining potential  $V(x, y)=V_L \exp[-(x+a)^2+y^2/\Delta^2]+V_R \exp[-(x-a)^2+y^2/\Delta^2]+V_p \exp[-x^2/\Delta_{px}^2-y^2/\Delta_{py}^2]$ . Here,  $V_L, V_R$  describe the depth of the left and right quantum dot minima located at  $x=-a, y=0$  and  $x=+a, y=0$ , and  $V_p$  is the plunger gate potential controlled by the central gate.<sup>26</sup> For identical dots,  $V_L=V_R=V_0$ , and confining potential exhibits inversion symmetry. Our numerical results are calculated for parameters based on (Cd,Mn)Te QDs with  $J_{sd}=0.015$  eV nm<sup>3</sup>,  $m^*=0.106$ ,  $\epsilon=10.6$ ,  $g_m=2.02$ , and  $g_e=-1.67$  and the effective Bohr radius  $a_B^*=5.29$  nm and Rydberg energy  $Ry^*=12.8$  meV. We parametrize the confining potential by  $V_0=-10$ ,  $a=2$ , and  $\Delta=2.5$  and  $\Delta_{px}=0.3$ ,  $\Delta_{py}=2.5$ , in effective atomic units.  $V_p$ , which controls the potential barrier, varies to control the interdot correlations, independent of the locations of the quantum dots. The choice of parameters ensures weakly coupled quantum dots.

## III. TWO LEVEL SYSTEM

For the purpose of this work, we consider a coupled quantum dot system filled with two electrons. It is convenient to project the Hilbert space of two electrons into a two level system. The construction of two level system based on single-particle orbitals localized in each dot is made by defining a pair of bonding-antibonding single-particle orbitals  $\varphi_{\pm}(\vec{r})=[\varphi_L(\vec{r}) \pm \varphi_R(\vec{r})]/\sqrt{2(1 \pm W)}$ , where  $\varphi_{L(R)}(\vec{r})$  is the spatial part of SP wave function localized in  $L$  ( $R$ ) dot, and  $W=\text{Re}\langle L|R\rangle$  is the overlap integral. At zero (finite) magnetic field, the SP orbitals are real (complex) functions. At  $H_{em}=B=0$  the lowest energy many body wave function (ground state) of two electrons is spatially symmetric with parity  $+1$ . Thus spin state of the ground state must be singlet:  $\Psi_G(\vec{r}_1, \vec{r}_2)=[\alpha\varphi_+(\vec{r}_1)\varphi_+(\vec{r}_2)+\beta\varphi_-(\vec{r}_1)\varphi_-(\vec{r}_2)]|S_0\rangle$ , where  $\beta=\sqrt{1-\alpha^2}$  and  $|S_0\rangle=(|\uparrow\downarrow\rangle-|\downarrow\uparrow\rangle)/\sqrt{2}$  corresponding to  $S=S_z=0$ . Here,  $S$  is the total spin of two electrons. The lowest energy excited states are the spin-triplet states with spatially antisymmetric wave function corresponding to parity  $-1$ , and  $\Psi_X^\sigma(\vec{r}_1, \vec{r}_2)=\frac{1}{\sqrt{2}}[\varphi_+(\vec{r}_1)\varphi_-(\vec{r}_2)-\varphi_+(\vec{r}_2)\varphi_-(\vec{r}_1)]|T_\sigma\rangle$ . Here,  $\sigma=0, \pm 1$ , and  $|T_\sigma\rangle$  is one of the spin-triplet states:  $|T_{+1}\rangle=|\uparrow\uparrow\rangle$ ,  $|T_0\rangle=(|\uparrow\downarrow\rangle+|\downarrow\uparrow\rangle)/\sqrt{2}$ , and  $|T_{-1}\rangle=|\downarrow\downarrow\rangle$  corresponding to  $S=1$ , and  $S_z=+1, 0, -1$ , respectively. Note that at  $B=0$  (or

zero Zeeman coupling) these states are degenerate and thus  $\Psi_X^\sigma$  is threefold degenerate. We define spin singlet-triplet energy gap of electrons  $\Delta_{ST}^{(e)} \equiv E_X^{(e)} - E_G^{(e)}$  where  $H_e|\Psi_G\rangle = E_G^{(e)}|\Psi_G\rangle$ , and  $H_e|\Psi_X^\sigma\rangle = E_X^{(e)}|\Psi_X^\sigma\rangle$ . In this two level system, there are two other excited states with spin-singlet  $\Psi_X^{s1}(\vec{r}_1, \vec{r}_2) = [\beta\varphi_+(\vec{r}_1)\varphi_+(\vec{r}_2) - \alpha\varphi_-(\vec{r}_1)\varphi_-(\vec{r}_2)]|S_0\rangle$ , and  $\Psi_X^{s2}(\vec{r}_1, \vec{r}_2) = \frac{1}{\sqrt{2}}[\varphi_+(\vec{r}_1)\varphi_-(\vec{r}_2) + \varphi_+(\vec{r}_2)\varphi_-(\vec{r}_1)]|S_0\rangle$ .

#### Weak $e$ -Mn coupling

Assuming the weak electron-Mn interaction limit, we calculate Mn-Mn effective Hamiltonian mediated by electrons perturbatively. In this limit  $H_{em}$  is assumed to be small, compared to unperturbed Hamiltonian  $H_e$ . In the low magnetic field limit, the ground state of two electrons in coupled quantum dot is spin-singlet. It follows:

$$H_{mm}^{\text{eff}} = \sum_X \frac{|\langle\Psi_X|H_{em}|\Psi_G\rangle|^2}{E_G^{(e)} - E_X^{(e)}}. \quad (5)$$

Here,  $G$  and  $X$  denote the ground and excited states of electrons in quantum dot systems, and  $X \in \{\Psi_X^{s1}, \Psi_X^{s2}, \Psi_X^{0,\pm 1}\}$ . The uniqueness (nondegeneracy) of the ground state has been assumed implicitly. To obtain effective interaction between two Mn, we calculate the matrix elements of  $H_{em}$ . It is straightforward to show that  $\langle\Psi_X^{s1}|H_{em}|\Psi_G\rangle = \langle\Psi_X^{s2}|H_{em}|\Psi_G\rangle = 0$ ,  $\langle\Psi_X^0|H_{em}|\Psi_G\rangle = \frac{\lambda J_{sd}}{2} \sum_I \Phi(\vec{R}_I) M_I^z$ ,  $\langle\Psi_X^{+1}|H_{em}|\Psi_G\rangle = -\frac{\lambda J_{sd}}{2} \sum_I \Phi(\vec{R}_I) M_I^+$ , and  $\langle\Psi_X^{-1}|H_{em}|\Psi_G\rangle = +\frac{\lambda J_{sd}}{2} \sum_I \Phi(\vec{R}_I) M_I^+$ , where  $\lambda = \alpha - \beta$  and  $\Phi(\vec{R}_I) \equiv \varphi_+(\vec{R}_I)\varphi_-(\vec{R}_I)$ . We finally find

$$H_{mm}^{\text{eff}} = \sum_{I,I'} \Delta_{II'} \vec{M}_I \cdot \vec{M}_{I'}, \quad (6)$$

where  $\Delta_{II'} = -\lambda^2 J_{sd}^2 / 2 \Delta_{ST}^{(e)} \varphi_+(\vec{R}_I)\varphi_-(\vec{R}_I)\varphi_+(\vec{R}_{I'})\varphi_-(\vec{R}_{I'})$ . Note that the Mn-Mn coupling for a lateral quantum dot molecule with two magnetic impurities localized at the center of each dot is given by

$$\Delta_{12} = + \frac{\lambda^2 J_{sd}^2 \varphi_L^2(\vec{R}_1)\varphi_R^2(\vec{R}_2)}{2 \Delta_{ST}^{(e)} 4(1 - W^2)} > 0. \quad (7)$$

Here, we assume that  $\vec{R}_1$  and  $\vec{R}_2$  are the position of Mn's centered at left and right dots, and therefore the electron wave functions at the opposite position of Mn's,  $\varphi_L^2(\vec{R}_2)$  and  $\varphi_R^2(\vec{R}_1)$  are negligible due to high localization of the wave functions. Because  $\Delta_{12}$  is positive, the coupling between two Mn mediated by electrons is antiferromagnetic with  $M=0$  as the ground state. For Mn, this state is separated by an energy gap,  $30\Delta_{12}$ , from the ferromagnetic state  $M=M_1+M_2(=5)$ . There are series of canted states with  $M=1, \dots, 4$  between  $M=0$  and  $M=5$ .

#### IV. EXACT DIAGONALIZATION

The effect of  $V_p$  at  $B=0$  on both  $\alpha$  and  $\Delta_{ST}^{(e)}$  is shown in Fig. 1. This calculation is based on configuration interaction (CI) method using 20 SP orbitals (400 electronic configurations). With increasing  $V_p$ , the interdot tunneling and the overlap between  $L$  and  $R$  wave functions decreases. This

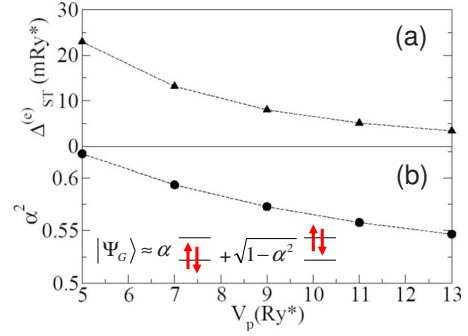


FIG. 1. (Color online) (a) Shown singlet-triplet energy gap ( $\Delta_{ST}^{(e)}$ ) of two electrons in a coupled quantum dot molecule as a function of plunger gate voltage ( $V_p$ ) at  $B=0$ . (b) Shown  $\alpha^2$  as a function of  $V_p$ .

results to the decrease of  $\alpha$  (hence  $\lambda$ ) and  $\Delta_{ST}^{(e)}$  simultaneously. The expansion of the ground state wave function  $|\Psi_G\rangle$ , in terms of leading configurations of two electrons is shown. The contribution of the rest of configurations is negligible.

With increase in magnetic field, the electron spin singlet-triplet energy gap  $\Delta_{ST}^{(e)}$  decreases. Close to the transition point,  $\Delta_{ST}^{(e)}$  vanishes, and the perturbation method fails. An unperturbative approach has to develop to calculate the low lying energy states of  $H$  in order to map  $H$  into  $H_{mm}^{\text{eff}}$ . Here we exactly diagonalize Hamiltonian  $H$  by expanding the many body wave function in the basis of electron-Mn configurations:  $|\Psi, M\rangle = c_{\alpha\sigma}^\dagger c_{\beta\sigma'}^\dagger |0\rangle \otimes |M_{z1}, M_{z2}\rangle$ . Because of  $[S_z, H_{em}] \neq 0$  ( $S$  is the total spin operator of two electrons), the states with different  $S_z$  are mixed, hence the dimension of matrix  $H$  that has to be diagonalized is given by  $N_C = (2M_1 + 1)(2M_2 + 1) \sum_{N_i=0}^N N_{SP}! / [N_\uparrow! (N_{SP} - N_\uparrow)!] N_{SP}! / [N_\downarrow! (N_{SP} - N_\downarrow)!]$ .  $N = N_\uparrow + N_\downarrow$  is the number of electrons (here  $N=2$ ), and  $N_{SP}$  is the number of single-particle orbitals. To check the convergence of CI we perform exact diagonalization using single-particle orbitals up to  $N_{SP}=20$ . The result of this calculation and the magnetic phase diagram of Mn is summarized in Fig. 2 where the electron spin singlet-triplet phase diagram is calculated by configuration interaction method for two electrons in lateral quantum dot molecules.

Figure 3 shows the lowest energy gap,  $\Delta = E_J - E_{J=0}$ , calculated for two electrons and two Mn in lateral quantum dot

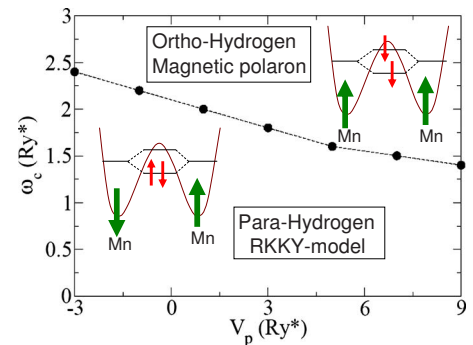


FIG. 2. (Color online) Spin singlet-triplet phase diagram calculated by configuration interaction method for two electrons in lateral quantum dot molecules.

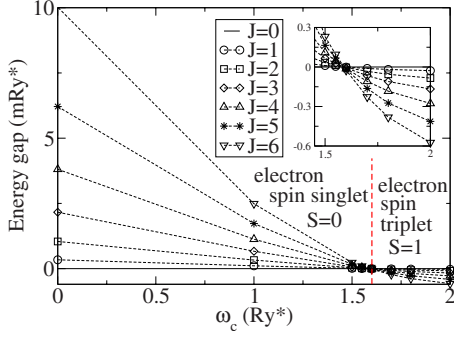


FIG. 3. (Color online) Energy gap of a system of two electrons and two Mn in lateral quantum dot molecule with  $V_p=7$  as a function of cyclotron energy (magnetic field). At  $\omega_c=1.55$  electron spin singlet-triplet transition is seen. The vertical dashed line marks the transition point. This transition induce para-ortho transition in Mn's. Below (above) this transition the ground state is identified by total angular momentum  $J=0$  ( $J=6$ ). A magnified part of main figure is shown in inset.

molecule as a function of cyclotron frequency  $\omega_c=eB/m^*c$  and  $J$ . Here  $\vec{J}=\vec{M}+\vec{S}$  is the total electron-Mn spin operator ( $\vec{M}=\vec{M}_1+\vec{M}_2$ , and  $\vec{S}=\vec{S}_1+\vec{S}_2$  are total Mn and electron spin operators). For illustration we switched off the electron and Mn-Zeeman couplings. Here the singlet-triplet transition occurs because of change in wave functions and  $e-e$  Coulomb matrix elements. Close to the transition point where the single-particle energy levels of valence electrons are degenerate (half-filled), the  $e-e$  Coulomb interaction leads singlet-triplet transition in accordance with spin Hund's rule. The eigenvalues of  $H$  are grouped into  $J=0, \dots, 6$ . States with given  $J$  are  $2J+1$ -fold degenerate. It is convenient to characterize these states based on the total spin of electrons, e.g., spin singlet ( $S=0$ ) and triplet ( $S=1$ ) and total spin of two Mn with  $M=0, \dots, 5$ . In this work, we are interested in the magnetic ordering of two Mn that can be described by antiferromagnetic, ferromagnetic, and canted states corresponding to  $M=0$ ,  $M=5$ , and  $M=1, \dots, 4$ . As it is shown in Fig. 3, spin of electrons undergo singlet-triplet transition at  $\omega_c^*=1.55$  and  $V_p=7$ . Within  $\omega_c < \omega_c^*$ ,  $J=M=S=0$  is the nondegenerate ground state. At  $\omega_c=\omega_c^*$ , the energy gap of antiferromagnetic, ferromagnetic, and canted states vanish all together and the ground state switches to ferromagnetic state with maximum spin multiplicity corresponding to  $J=6$ ,  $M=5$ , and  $S=1$ . In the limit of strong magnetic field, there are  $2J+1=13$  degenerate states that form the ground state. However, this degeneracy is removed by Zeeman coupling that guarantees the uniqueness of the ground state with  $M_z=-5$  and  $S_z=-1$ . Within the resolution of our exact diagonalization we did not observe any range of magnetic field that the ground state exhibits canted ordering. In Fig. 3 at  $B=0$  and  $V_p=7$  we

compare the energy gap calculated using CI,  $E_{J=6}-E_{J=0}=10$  mRy\*, with perturbation approach. We find  $\Delta_{ST}^{(e)}=0.013$ ,  $\Delta_{12}=0.38$ , hence  $E_{J=6}-E_{J=0}=11.4$  all in mRy\*, in qualitative agreement with exact energy gap.

## V. CONCLUSION

In this work we studied phase diagram of quantum dot molecules consists of two electrons and two magnetic impurities (Mn) confined in each dot. We demonstrated that the spin singlet-triplet transition of two electrons that are controlled by external electric gate voltage and magnetic field, can induce ferromagnetic-antiferromagnetic transition in the magnetic impurity system. Therefore, Mn-Mn spin transitions mediated by ( $e$ -Mn) exchange interaction can be controlled indirectly by external electric gate voltage and magnetic field. This allows us to suggest application of spin of magnetic impurities for the entanglement of qubits in quantum information processing. The advantage of using spin of magnetic impurities as qubit, instead of QD electrons resides in the possibility of achieving higher spin coherence time. In analogous to the magnetic moment of nuclear impurities in host semiconductor systems, we speculated that the spin coherence time in the Mn system is expected to be longer than the QD electron system due to small localization length of Mn  $d$ -orbitals that suppresses the qubit spin-orbit coupling as well as hyperfine interaction with the magnetic moment of nuclei of host semiconductor.

Our analysis based on exact diagonalization allows mapping the electron-electron and electron-Mn Hamiltonian  $H$  into an effective Mn-Mn Heisenberg Hamiltonian  $H_{mm}^{\text{eff}}=\Delta_{12}\vec{M}_1\cdot\vec{M}_2$  in agreement with the perturbative results, e.g., an RKKY model calculated for weak coupling at low magnetic fields. Consistent with the magnetic field dependence of the lowest lying states of full Hamiltonian  $H$ ,  $\Delta_{12}$  changes sign at critical magnetic field that leads to spin singlet-triplet transition of two electrons in lateral quantum dot molecules. This is a level crossing that results to para-ortho transition induced by electrons in artificial  $H_2$  molecules where the magnetic impurities resembling the magnetic moment of nucleus of the actual  $H_2$  molecules. The interaction between two Mn at high magnetic field is determined by the magnetic polaron effect.

## ACKNOWLEDGMENTS

Author acknowledges partial support from the U.S. ONR under Grants No. N00014-06-1-0616 and No. N00014-06-1-0123, and NSF ECCS, and thanks Thomas Brabec, Sasha Govorov, Pawel Hawrylak, Miguel Angel Martin-Delgado, Andre Petukhov, Dean Sherry, and Igor Zutic for comments and discussions.



- <sup>1</sup>L. Jacak, P. Hawrylak, and A. Wojs, *Quantum Dots* (Springer, Berlin, 1998); D. Bimberg, M. Grundmann, and N. N. Ledentsov, *Quantum Dot Heterostructures* (Wiley, Chichester, 1999); S. M. Reimann and M. Manninen, *Rev. Mod. Phys.* **74**, 1283 (2002), and the references therein.
- <sup>2</sup>L. Besombes, Y. Leger, L. Maingault, D. Ferrand, H. Mariette, and J. Cibert, *Phys. Rev. Lett.* **93**, 207403 (2004); *Phys. Rev. B* **71**, 161307(R) (2005); C. Le Gall, L. Besombes, H. Boukari, R. Kolodka, J. Cibert, and H. Mariette, *Phys. Rev. Lett.* **102**, 127402 (2009); Y. Leger, L. Besombes, J. Fernandez-Rossier, L. Maingault, and H. Mariette, *ibid.* **97**, 107401 (2006); Y. Leger, L. Besombes, L. Maingault, D. Ferrand, and H. Mariette, *ibid.* **95**, 047403 (2005).
- <sup>3</sup>C. Gould, A. Slobodskyy, D. Supp, T. Slobodskyy, P. Grabs, P. Hawrylak, F. Qu, G. Schmidt, and L. W. Molenkamp, *Phys. Rev. Lett.* **97**, 017202 (2006).
- <sup>4</sup>Tak Gurung, Sebastian Mackowski, Grzegorz Karczewski, Howard E. Jackson, and Leigh M. Smith, *Appl. Phys. Lett.* **93**, 153114 (2008).
- <sup>5</sup>D. A. Bussian, *Nature Mater.* **8**, 35 (2009).
- <sup>6</sup>J. van Bree, P. M. Koenraad, and J. Fernandez-Rossier, *Phys. Rev. B* **78**, 165414 (2008).
- <sup>7</sup>D. E. Reiter, T. Kuhn, and V. M. Axt, *Phys. Rev. Lett.* **102**, 177403 (2009).
- <sup>8</sup>J. Fernandez-Rossier and L. Brey, *Phys. Rev. Lett.* **93**, 117201 (2004).
- <sup>9</sup>A. O. Govorov, *Phys. Rev. B* **72**, 075359 (2005); Wei Zhang, T. Dong, and A. O. Govorov, *ibid.* **76**, 075319 (2007).
- <sup>10</sup>F. Qu and P. Hawrylak, *Phys. Rev. Lett.* **96**, 157201 (2006).
- <sup>11</sup>R. M. Abolfath, A. Petukhov, and I. Zutic, *Phys. Rev. Lett.* **101**, 207202 (2008); R. M. Abolfath, P. Hawrylak, and I. Zutic, *ibid.* **98**, 207203 (2007); *New J. Phys.* **9**, 353 (2007).
- <sup>12</sup>S.-J. Cheng, *Phys. Rev. B* **79**, 245301 (2009).
- <sup>13</sup>Nga T. T. Nguyen and F. M. Peeters, *Phys. Rev. B* **78**, 045321 (2008); **78**, 245311 (2008).
- <sup>14</sup>C. Echeverria-Arrondo, J. Perez-Conde, and A. Ayuela, *Phys. Rev. B* **79**, 155319 (2009).
- <sup>15</sup>T. H. Oosterkamp, S. F. Godijn, M. J. Uilenreep, Y. V. Nazarov, N. C. van der Vaart, and L. P. Kouwenhoven, *Phys. Rev. Lett.* **80**, 4951 (1998); M. Ciorga, A. Wensauer, M. Pioro-Ladriere, M. Korkusinski, J. Kyriakidis, A. S. Sachrajda, and P. Hawrylak, *ibid.* **88**, 256804 (2002); M. Pioro-Ladriere, M. Ciorga, J. Lapointe, P. Zawadzki, M. Korkusinski, P. Hawrylak, and A. S. Sachrajda, *ibid.* **91**, 026803 (2003); J. R. Petta, A. C. Johnson, C. M. Marcus, M. P. Hanson, and A. C. Gossard, *ibid.* **93**, 186802 (2004); M. Pioro-Ladriere, R. Abolfath, P. Zawadzki, J. Lapointe, S. A. Studenikin, A. S. Sachrajda, and P. Hawrylak, *Phys. Rev. B* **72**, 125307 (2005).
- <sup>16</sup>G. Burkard, D. Loss, and D. P. DiVincenzo, *Phys. Rev. B* **59**, 2070 (1999); X. Hu and S. Das Sarma, *Phys. Rev. A* **64**, 042312 (2001); R. M. Abolfath, W. Dybalski, and P. Hawrylak, *Phys. Rev. B* **73**, 075314 (2006).
- <sup>17</sup>L. Cywinski, W. M. Witzel, and S. DasSarma, *Phys. Rev. Lett.* **102**, 057601 (2009); W. A. Coish and D. Loss, *Phys. Rev. B* **72**, 125337 (2005).
- <sup>18</sup>D. G. Cory, M. D. Price, W. Maas, E. Knill, R. Laflamme, W. H. Zurek, T. F. Havel, and S. S. Somaroo, *Phys. Rev. Lett.* **81**, 2152 (1998); M. A. Nielsen, E. Knill, and R. Laflamme, *Nature (London)* **396**, 52 (1998).
- <sup>19</sup>B. E. Kane, *Nature (London)* **393**, 133 (1998); A. Galindo and M. A. Martin-Delgado, *Rev. Mod. Phys.* **74**, 347 (2002).
- <sup>20</sup>H. O. H. Churchill, F. Kueemmeth, J. W. Harlow, A. J. Bestwick, E. I. Rashba, K. Flensberg, C. H. Stwertka, T. Taychatanapat, S. K. Watson, and C. M. Marcus, *Phys. Rev. Lett.* **102**, 166802 (2009); J. Fischer, B. Trauzettel, and D. Loss, *Phys. Rev. B* **80**, 155401 (2009).
- <sup>21</sup>M. Carravetta, O. G. Johannessen, and M. H. Levitt, *Phys. Rev. Lett.* **92**, 153003 (2004); W. S. Warren, Elizabeth Jenista, Rosa Tamara Branca, and Xin Chen, *Science* **323**, 1711 (2009).
- <sup>22</sup>J. Almeida, M. A. Martin-Delgado, and G. Sierra, *Phys. Rev. B* **79**, 115141 (2009) and references therein.
- <sup>23</sup>M. A. Ruderman and C. Kittel, *Phys. Rev.* **96**, 99 (1954); T. Kasuya, *Prog. Theor. Phys.* **16**, 45 (1956); K. Yosida, *Phys. Rev.* **106**, 893 (1957).
- <sup>24</sup>L. D. Landau and E. M. Lifshitz, *Quantum Mechanics: Non-Relativistic Theory* (Pergamon, Oxford, 2003).
- <sup>25</sup>Because the nuclear wave function of H<sub>2</sub> molecule is odd under exchange of two protons, in the gas phase, the para and ortho energy gap can be expressed as the energy difference between nuclear rotational energy levels associated with the molecular angular momentum. In the solid phase, the rotational degree of freedom of H<sub>2</sub> molecules is frozen, and the para and ortho states of hydrogen are degenerate. The spin degeneracy is removed by the electron-proton hyperfine interaction that is analogous to the *e*-Mn contact interaction in artificial H<sub>2</sub> quantum dot molecule.
- <sup>26</sup>R. M. Abolfath and Pawel Hawrylak, *J. Chem. Phys.* **125**, 034707 (2006).
- <sup>27</sup>W. A. Coish and J. Baugh, *Phys. Status Solidi B* **246**, 2203 (2009).
- <sup>28</sup>G. Dresselhaus, *Phys. Rev.* **100**, 580 (1955); E. I. Rashba, *Fiz. Tverd. Tela (Leningrad)* **2**, 1224 (1960) [*Sov. Phys. Solid State* **2**, 1109 (1955)]; Y. A. Bychkov and E. I. Rashba, *J. Phys. C* **17**, 6039 (1984).